

# Search for binary central stars of the SMC PNe<sup>★</sup>

M. Hajduk<sup>1</sup>, M. Gładkowski<sup>1,2</sup>, and I. Soszyński<sup>3</sup>

<sup>1</sup> Nicolaus Copernicus Astronomical Center, ul. Rąbiana 8, 87-100 Toruń, Poland

<sup>2</sup> Centrum Astronomii UMK, ul. Gagarina 11, 87-100 Toruń, Poland

<sup>3</sup> Warsaw University Observatory, Al. Ujazdowskie 4, 00-478 Warszawa, Poland

Received ; accepted

## ABSTRACT

**Aims.** The Optical Gravitational Lensing Experiment (OGLE), originally designed to search for microlensing events, provides a rich and uniform data set suitable for studying the variability of certain types of objects. We used the OGLE data to study the photometry of central stars of planetary nebulae (PNe) in the Small Magellanic Cloud (SMC). In particular, we searched for close binary central stars with the aim to constrain the binary fraction and period distribution in the SMC. We also searched for PNe mimics and removed them from the PNe sample.

**Methods.** We identified 52 counterparts of PNe in the SMC in the I-band images from the OGLE-II and OGLE-III surveys. We analysed the time-series photometry of the PNe. Spectra of the photometric variables were obtained to constrain the nature of the objects or search for additional evidence for binarity.

**Results.** Eight variables were found. Of these, seven objects are PNe mimics, including one symbiotic star candidate. One close binary central star of PN with a period of 1.15 or 2.31 day was discovered. The obtained binary fraction for the SMC PNe and the observational biases are discussed in terms of the OGLE observations.

**Key words.** ISM: planetary nebulae: general – stars: binaries: general – stars: binaries: symbiotic – galaxies: Magellanic Clouds

## 1. Introduction

Large-scale photometric surveys provide an excellent opportunity to improve our understanding of the nature of the planetary nebula (PN) phenomenon. Using large photometric surveys allowed researchers to monitor the brightness of hundreds of central stars of planetary nebulae (CSPNe, Miszalski et al. 2009a; Lutz et al. 2010; Jones et al. 2011; Hajduk et al. 2011). The number of known binary CSPNe was more than doubled in recent years (De Marco 2011). The fraction of close binary CSPNe was established as 12-21% on the basis of the Optical Gravitational Lensing Experiment (OGLE) photometry in the Galactic Bulge (Miszalski et al. 2009a), consistent with the 10-15% fraction given by Bond (2000).

The growing number of binary CSPNe made it possible to compare the period distribution with the population synthesis model predictions and to study the influence of the common envelope (CE) phase of the binary evolution on the morphology of the nebulae (De Marco 2009; Miszalski et al. 2009a,b; Boffin et al. 2012).

Here, we present OGLE-II and OGLE-III observations of the Small Magellanic Cloud (SMC) PNe (Udalski et al. 1997, 2008). We report the discovery of one binary nucleus. Seven objects are confirmed to be PN mimics, including a symbiotic mira candidate.

## 2. PNe sample

SMC PNe were selected using the SIMBAD database. We made use of the object type and coordinate search criteria and

found 108 objects. The list includes PNe discovered by Lindsay (1961), Sanduleak et al. (1978), Sanduleak & Pesch (1981), Morgan & Good (1985), Morgan (1995), and Meyssonnier (1995) by means of objective-prism plates or long-slit spectroscopy. Jacoby & De Marco (2002) used narrow-band imaging, but subsequently confirmed their sample with spectroscopic follow-up. Jacoby (1980) used on-line/off-line filter photography. Their sample was spectroscopically verified by Boroson & Liebert (1989), who showed that 30% of Jacoby's PNe candidates could not be confirmed or have other explanations.

We supplemented our list with nine PNe confirmed by Morgan (1995) and one from Sanduleak et al. (1978), which were missing from the Simbad database. We also included one object from Jacoby & De Marco (2002), classified as a He-burning asymptotic giant branch (AGB) star in the Simbad database. The total sample comprises 119 objects.

The objects were identified by visual comparison of the finding charts available in the literature with the OGLE-II and OGLE-III I-band reference images. In addition, we observed 27 objects in the SMC with the 1.0m telescope at the South African Astronomical Observatory (SAAO) with the R and H $\alpha$  filters. No H $\alpha$  emission was identified in three cases (Jacoby SMC 12, Jacoby SMC 15 and [JD2002]3). Jacoby SMC 12 and Jacoby SMC 15 were misclassified as PNe (Boroson & Liebert 1989). [JD2002]3 shows faint, extended nebula, probably below the sensitivity of our H $\alpha$  image (Jacoby & De Marco 2002).

We identified 52 objects in the OGLE reference images in total out of 119 candidates (Table 1 and 2). Though all the PNe in the sample were spectroscopically confirmed, classification of eight objects was ambiguous (Table 2). [MA93]22 was classified as a PN (Meyssonnier 1995) even though it shows a strong

\* Table 4 is only available in electronic form at the CDS via anonymous ftp to cdsarc.u-strasbg.fr (130.79.128.5) or via <http://cdsweb.u-strasbg.fr/cgi-bin/qcat?J/A+A/>

**Table 1.** List of PNe identified in the OGLE-II and OGLE-III fields in the SMC. Column  $N_I$  gives the number of the OGLE-II (when available) and OGLE-III observations.

name	RA	DEC	V	I	$N_I$	ref	diameter [arcsec]	other names
LHA 115-N 4	0 34 21.99	-73 13 21.4	16.809	18.464	700	[1]	0.54 [11]	LIN 16, SMP 3
LHA 115-N 5	0 41 21.68	-72 45 16.7	15.805	17.224	705	[1]		LIN 32, SMP 5, [MA93] 23
LHA 115-N 6	0 41 27.75	-73 47 06.5	15.916	16.942	1213	[1]	... [10]	SMP 6, LIN 33, [MA93] 29
Jacoby SMC 1	0 42 28.15	-73 20 55.1	18.230	19.598	603+671	[2]		SMP 7, [MA93] 39
[MA93] 44	0 43 09.40	-73 08 03.7	19.803	20.487	307+655	[6]		
LHA 115-N 7	0 43 25.32	-72 38 18.9	16.212	17.365	705	[1]	0.41 × 0.38 [10]	LIN 43, SMP 8, [MA93] 49
MGPn SMC 6	0 44 25.73	-73 51 39.3	20.417	20.535	1143	[7]		[MA93] 73
[JD2002] 1	0 45 12.10	-73 18 58.0	20.487	20.445	308+682	[9]		
LIN 66	0 45 20.65	-73 24 10.3	17.494	19.155	399+697	[5]	1.20 [10]	J3, SMP 9, [MA93] 98
LIN 71	0 45 27.43	-73 42 14.5	15.659	14.505	1215	[5]	0.27 [10]	[MA93] 104, J4
[JD2002] 2	0 45 36.66	-73 24 04.3	17.993	17.881	322+697	[9]		
[JD2002] 5	0 47 39.99	-72 39 03.0	19.443	19.425	753	[9]		
LHA 115-N 29	0 48 36.55	-72 58 00.9		16.715	298+723	[1]	0.78 × 0.66 [10]	SMP 11, LIN 115, [MA93] 241, J8
[JD2002] 6	0 49 08.24	-73 02 23.6	19.336	19.290	337+722	[9]		
Jacoby SMC 9	0 49 20.11	-73 17 35.3	19.817	19.881	334+30	[3]		[MA93] 290
SMP SMC 12	0 49 21.10	-73 52 58.7	18.536	17.983	354	[4]		[MA93] 291
[JD2002] 7	0 49 35.44	-73 26 33.7	19.835	18.868	325+545	[9]		
[M95] 3	0 49 47.47	-74 14 40.0	17.663	17.859	694	[8]		
LHA 115-N 38	0 49 51.65	-73 44 21.4	15.382	16.913	547	[1]		
LHA 115-N 40	0 50 35.09	-73 42 58.1	16.500	18.095	700	[1]	0.83 [10]	
[MA93] 406	0 50 52.38	-73 44 55.2	18.574	19.751	691	[6]		
LHA 115-N 43	0 51 07.38	-73 57 37.6	15.341	16.444	709	[1]	0.32 [11]	SMP 15, LIN 174 [MA93] 433
[JD2002] 12	0 51 07.82	-73 12 06.4	18.330	17.349	337+722	[9]	1.15 × 1.40 [11]	
LHA 115-N 42	0 51 27.17	-72 26 11.7	16.741	16.922	753	[1]	0.33 × 0.30 [11]	LIN 179, SMP 16, J14, [MA93] 467
LHA 115-N 47	0 51 58.13	-73 20 31.3	16.158	16.626	339+713	[1]	0.14 [10]	LIN 196, [MA93] 519, J19, SMP 18
LIN 239	0 53 11.13	-72 45 07.5	16.432	17.873	321+752	[5]	0.59 [10]	J20, SMP 19, [MA93] 652
[MA93] 891	0 55 59.42	-72 14 00.8	19.274	20.314	712	[6]		
LIN 302	0 56 19.48	-72 06 58.4	17.609	17.792	721	[5]	1.39 × 1.28 [10]	MGPn 8, [MA93] 933
LIN 305	0 56 30.77	-72 27 02.1	17.181	18.023	209+617	[5]		[MA93] 943, SMP 21
[JD2002] 17	0 56 52.53	-72 21 02.3	19.968	19.129	661	[9]		
LIN 343	0 58 42.32	-72 56 59.8	16.910	18.387	307+713	[5]	0.66 × 0.60 [10]	J26, SMP 23, [MA93] 1088
LHA 115-N 68	0 58 43.04	-72 27 16.2		18.920	288+712	[1]		[MA93] 1091, LIN 339, MGPn 9
LHA 115-N 70	0 59 16.12	-72 02 00.0	16.016	16.916	721	[1]	0.38 [10]	SMP 24, [MA93] 1136, LIN 347
[JD2002] 19	0 59 29.37	-73 39 05.9	20.943	20.641	631	[9]		
LIN 357	0 59 40.51	-71 38 15.1	17.856	18.581	704	[5]		SMP 25, [MA93] 1159
[JD2002] 20	1 00 15.11	-72 16 40.7	20.567	21.140	541	[9]		
[JD2002] 23	1 02 00.91	-72 59 02.0	20.560	20.783	313+463	[9]		
[MA93] 1438	1 04 04.69	-71 37 24.9	20.320	20.421	669	[6]		
LIN 430	1 04 17.90	-73 21 51.1	18.124	19.151	737	[5]	0.61 × 0.57 [10]	SMP 26, [MA93] 1454
[MA93] 1709	1 09 51.84	-73 20 50.6	19.457	18.657	735	[6]		
[MA93] 1714	1 10 04.86	-72 45 27.5	19.342	18.411	675	[6]		
SMP SMC 34	1 12 10.86	-71 26 50.6	18.584	19.771	648	[4]	0.71 × 0.69 [10]	[MA93] 1757
[MA93] 1762	1 12 40.25	-72 53 46.8	20.109	20.309	90	[6]	1.45 × 1.26 [10]	
LHA 115-N 87	1 21 10.65	-73 14 34.8	15.553	16.758	637	[1]	0.45 [10]	LIN 532, SMP 27, [MA93] 1884
LIN 536	1 24 11.85	-74 02 32.2	17.589	17.716	625	[5]	0.31 [11]	SMP 28

References: [1] Henize (1956), [2] Sanduleak et al. (1978), [3] Jacoby (1980), [4] Sanduleak & Pesch (1981), [5] Lindsay (1961), [6] Meyssonnier & Azzopardi (1993), [7] Morgan & Good (1985), [8] Morgan (1995), [9] Jacoby & De Marco (2002), [10] Stanghellini et al. (2003), [11] Shaw et al. (2006)

continuum and a very weak [O III] 5007Å line. Haberl & Sasaki (2000) classified it as a Be/X-ray binary. The PN nature of LIN 34 and Jacoby SMC 7 was questioned by Morgan (1995). The former object was classified as a B0-5V star by Evans et al. (2004). Jacoby SMC 23 is a young stellar object (YSO) candidate (Bolatto et al. 2007) and Jacoby SMC 24 is probably an H II region (Borosen & Liebert 1989). Henize & Westerlund (1963) classified LHA 115-N 9, LHA 115-N 61, and LHA 115-N 68 as diffuse nebulae. But we classify LHA 115-N 68 as a PN, since it shows a prominent [O III] 5007Å line (Leisy & Dennefeld 2006). [JD2002] 11 was classified as an extreme AGB star candidate on

the basis of the infrared colour-magnitude diagram (Boyer et al. 2011).

Seven known PN mimics show photometric variability. We present here the spectroscopy and photometry of these objects in addition to the genuine PNe to study their characteristics (which may be of interest to other research groups) in an endeavour to understand their nature, before ultimately rejecting them from the PN sample.

**Table 2.** List of the PNe mimics showing photometric variability.

name	RA	DEC	V	I	$N_I$	ref	diameter [arcsec]	other names
[MA93] 22	0 41 09.13	-73 06 47.1	17.796	17.764	304+691	[4]		
LIN 34	0 42 15.77	-72 59 55.4	16.441	16.450	315+537	[3]		[MA93] 37
LHA 115-N 9	0 43 36.69	-73 02 26.9	15.529	15.883	317+698	[1]		[MA93] 54, LIN 45
Jacoby SMC 7	0 48 05.36	-73 09 05.9	19.278	18.947	324+722	[2]		
[JD2002] 11	0 50 52.66	-72 52 16.7	21.263	19.562	333+722	[6]		
Jacoby SMC 23	0 55 30.42	-72 50 21.9	18.358	17.835	295+713	[5]	... [7]	[MA93] 852
Jacoby SMC 24	0 56 39.40	-72 39 07.2	17.920	16.619	295+713	[2]		[MA93] 955

References: [1] Henize & Westerlund (1963), [2] Boroson & Liebert (1989), [3] Morgan (1995), [4] Haberl & Sasaki (2000), [5] Bolatto et al. (2007), [6] Boyer et al. (2011), [7] Stanghellini et al. (2003)

**Table 3.** Spectroscopic observations of objects showing photometric variability.

date	telescope	exptime [s]	name
2012-09-17	SALT	120	Jacoby SMC 24
2012-09-19	SALT	120+1200	Jacoby SMC 23
2012-09-19	SALT	2 × 120+1200	Jacoby SMC 1
2012-10-10	SALT	120+1200	Jacoby SMC 1
2012-11-25	SALT	900	Jacoby SMC 7
2012-11-26	SALT	900	[JD2002] 11
2013-07-17	Radcliffe	2 × 1800	LHA 115-N 61
2013-07-21	Radcliffe	3 × 1200	LIN 34
2013-07-21	Radcliffe	2 × 1200	[MA93] 22

### 3. Observations

We used the V- and I-band photometry of the SMC collected by the OGLE-III project. OGLE-II photometry was available for some of the objects as well. The V-band photometry was obtained only intermittently, while I-band observations were made frequently. The I-band filter had a wide long-wavelength wing, quite different from the sharp drop of transmission at about 9000Å of the standard I-bandpass (Udalski et al. 2002). The data were taken only under good seeing conditions. The median seeing during the observations of the SMC was equal to 1.''2 (Udalski et al. 2008).

The photometry of some objects is affected by systematic effects, which hampers the time-series analysis. This problem was previously reported by Miszalski et al. (2009a) for CSPNe suffering from strong nebular contamination. We examined OGLE I-band images of our objects. Only two of them are clearly resolved: LHA 115-N 9 and LHA 115-N 61, both classified as diffuse nebulae (Section 2). Some other objects have full width at half maximum (FWHM) that is somewhat larger than that of the field stars.

Eight objects were found to be variable. We performed spectroscopic observations of five variables with the Southern African Large Telescope (SALT), and three variables were observed with the Radcliffe 1.9m telescope at SAAO (Table 3). The SALT low-resolution spectra were obtained with the 900l/mm grating. The slit was 1 arcsec wide and 8 arcmin long. The spectral coverage was 4350-7400Å with the spectral resolution of about  $\lambda/\Delta\lambda = 6000$  at the central wavelength. A 2 arcsec wide slit and the 300l/mm grating was used for the 1.9m telescope, resulting in the spectral resolution of about 2500 at the central wavelength. The spectral coverage was set to 3500-7500Å. All the spectra were flux calibrated.

### 4. Results

We analysed the OGLE-II and OGLE-III I-band photometry using the program Period04 (Lenz & Breger 2005) and the analysis of variance (ANOVA) method (Schwarzenberg-Czerny 1996). We identified six periodic variables (including one with a period of about 4.5 years) and two irregular variables. The phased light curves of the all periodic variables are presented in Figure 1. The irregular light curves and periodic light curves with periods long enough to be legible are shown in Figure 2. The spectra of all the variable objects but [MA93] 22 are presented in Figure 3. All the spectra are available at CDS (Table 4).

Out of the total sample of eight variable objects detected, we considered seven objects to be PNe mimics. They have previously been suggested to be PNe mimics or were considered as objects of uncertain nature. One remaining (periodic) variable is most likely a genuine binary CSPN.

#### 4.1. Variable stars

LIN 34 has a period of  $1.67886 \pm 0.00007$  day (Figure 1). It is catalogued as a PN, but Meyssonnier & Azzopardi (1993) classified it as a very low excitation (VLE) object. The spectrum of LIN 34 is characterised by strong continuum and lack of obvious [O III] 5007Å emission (Figure 3). The observed wavelength of the emission lines corresponds to a radial velocity of about  $-30 \text{ km s}^{-1}$ , thus LIN 34 appears to be a pulsating Galactic halo Be star (Greenstein & Sargent 1974).

[MA93] 22 was classified as a PN by Meyssonnier (1995), although its spectrum revealed a strong continuum and a very weak [O III] 5007Å line. The object shows variability on a timescale of about 1630 days (Figure 2). Three maxima were covered by the OGLE-II and -III phase observations. The last maximum is fainter than the first two maxima by about 0.1 mag, which affected the appearance of the phased light curve of the object (Figure 1). The object showed only a weak H $\alpha$  emission in a very noisy 1.9m telescope spectrum, not shown in Figure 3. [MA93] 22 was proposed as the optical counterpart of an X-ray binary afterwards (Haberl & Sasaki 2000). It is clearly detected in the 2MASS K band, but not detected in the J and H bands. The near-IR emission lines may significantly contribute to the brightness of the object in the K band (Naik et al. 2012). The optical variability could correspond to the orbital period of the binary.

[JD 2002] 11 has a period of  $215.3 \pm 0.2$  days (Figure 1). The [O III] 5007Å emission line is detected in the spectrum, exceeding the H $\beta$  line in intensity (Figure 3). [JD 2002] 11 probably is a symbiotic system. The 215.3 day period may be due to the pulsation of the cool component, while the hot component is re-

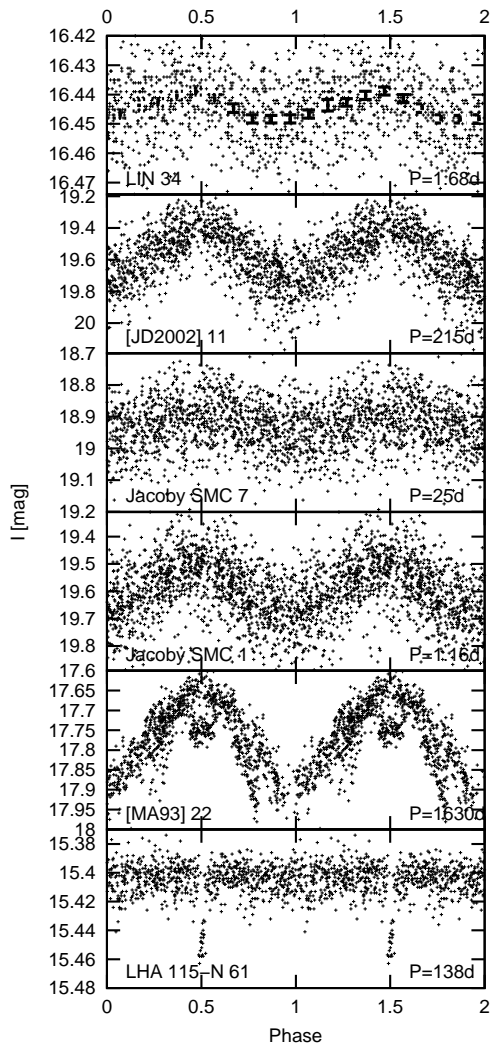


**Fig. 1.** Phased OGLE I-band light curves of the SMC periodic variables.

sponsible for the ionization of the nebula. However, the quality (and wavelength range) of the spectrum did not allow us to unveil the spectral signature of the cool component.

Near-infrared photometry allows one to separate genuine PNe from symbiotic miras (Schmeja & Kimeswenger 2001). PNe are located in a well-defined region in the IJK two-colour diagram. We searched for the Two Micron All Sky Survey (2MASS) photometry of all the PNe identified in the SMC (Skrutskie et al. 2006). Infrared colours confirm that [JD 2002] 11 is a symbiotic mira and not a PN (Figure 4). If the classification is correct, then [JD2002] 11 would be only the eight symbiotic star discovered in the SMC (Belczyński et al. 2000; Oliveira et al. 2013).

Jacoby SMC 7 has a period of  $24.93 \pm 0.01$  days (Figure 1). The object was disclaimed to be a genuine PN by Boroson & Liebert (1989). It is located in an extended [O III]  $5007\text{\AA}$  and H I emission region of the supernova remnant (SNR) [FBR2002] J004806-730842. The spectrum of Jacoby SMC 7 contains H I lines, but the [O III]  $5007\text{\AA}$  emission was extracted with the diffuse background emission of the SNR (Figure 3). Mennickent et al. (2002) observed a group of Be stars charac-

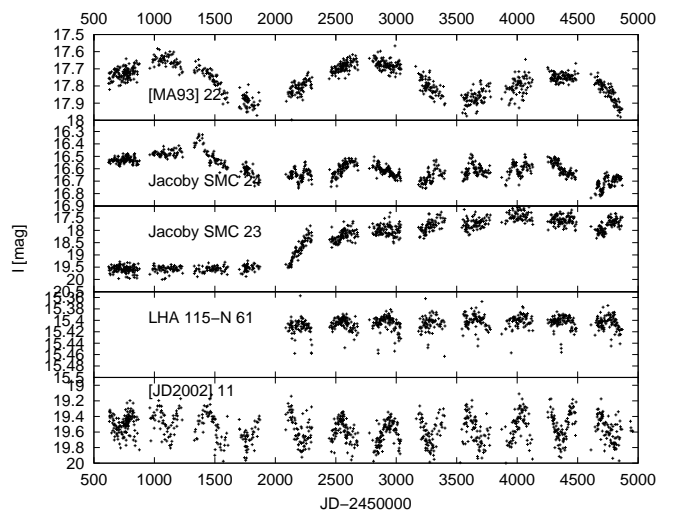


**Fig. 2.** OGLE-II and -III photometry of the variable objects with periods long enough to be readily presented.

terized by periods longer than 17 days. Jacoby SMC 7 may be a new member of this group.

Jacoby SMC 23 lies on the edge of an open cluster OGLE-CL SMC 104. The object experienced a sudden flux increase during the first season of the OGLE-III operation (Figure 2). No variability was found before that event. No significant colour change accompanied the outburst. The object shows wide H $\alpha$  line wings in the spectrum (Figure 3), which were previously reported by Stanghellini et al. (2003). Jacoby SMC 23 is most likely a YSO experiencing an increase of the accretion rate. It may be an optical counterpart of the YSO candidate S3MC J005530.39-725021.87 (Bolatto et al. 2007).

The spectrum of Jacoby SMC 24 shows only H $\alpha$  and H $\beta$  lines (Figure 3). The light curve reveals irregular or semi-regular variations (Figure 2). We do not consider this object as a genuine PN. The nature of this PN candidate was previously debated by Morgan & Good (1985) and the object was not recovered by Jacoby & De Marco (2002). The light curve showing stochastic variability is similar to the light curves of most of the Be stars in the SMC (Mennickent et al. 2002).

LHA 115-N61 shows eclipses lasting for three days with a period of about 138 days (Figure 1). The light curve shows an additional 183-day variability (half a year) of instrumental origin (Figure 2). There is no OGLE-II photometry of the source available since it was resolved by the pipeline. The object was suggested to be a diffuse nebula by Henize & Westerlund (1963), because it was brighter than other SMC PNe and resolved. The observed [O III]  $5007\text{\AA}$ /H $\beta$  flux ratio is of the order of unity, which may suggest a PN excited by a young central star. However, in that case the nebula would be compact and unresolved. The nebula is most likely excited by an eclipsing binary system of O V type stars. The depth of the eclipses may be suppressed by the nebular contribution.

Jacoby SMC 1 is a binary CSPN with a period of  $1.15539 \pm 0.00001$  days assuming the irradiation effect to be the cause of the variations, or twice that period in the case of ellipsoidal variations (Figure 1). The observed amplitude of the variations is about 0.3 magnitude, but may be suppressed by the nebular contribution to the I brightness. The spectrum, showing strong [O III]  $5007\text{\AA}$  emission and faint, blue continuum, strongly supports that the object is a genuine PN. However, we did not detect any irradiation lines coming from the cool component (Figure 3),

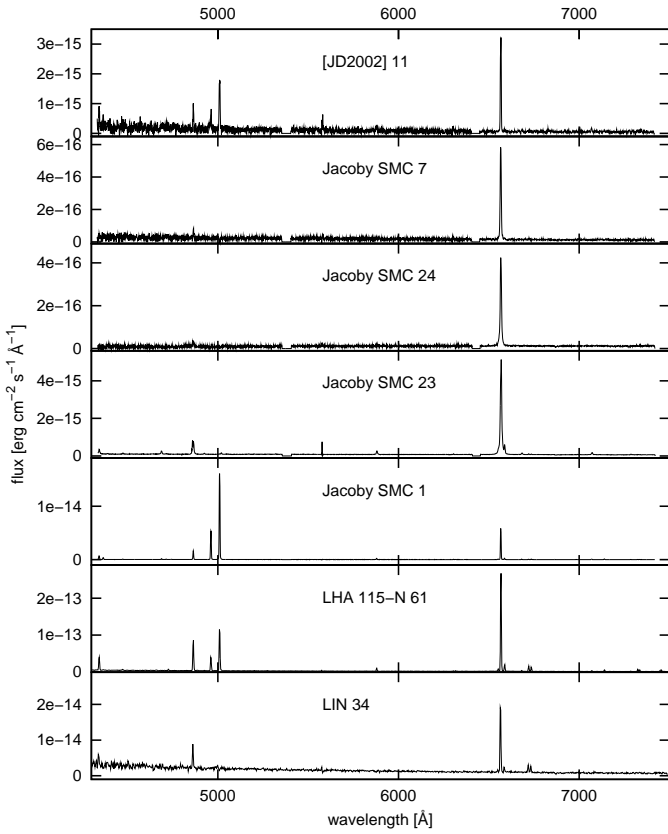


**Fig. 3.** Spectra of the variable objects.

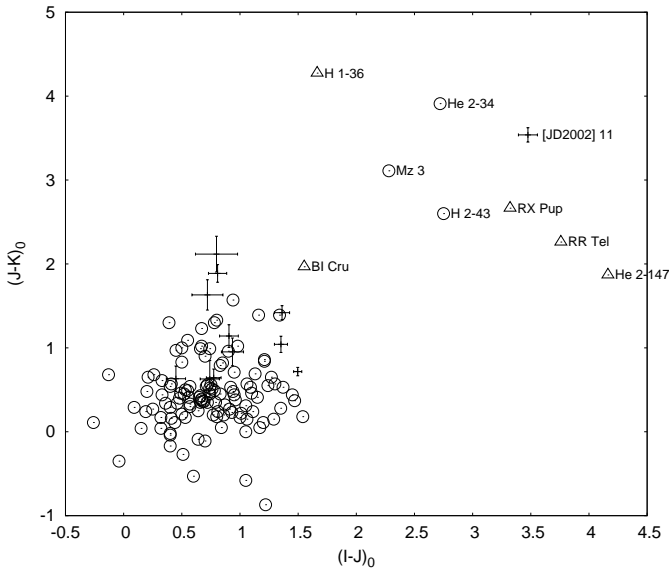


**Fig. 4.** IJK two-colour diagnostic diagram for the Galactic and SMC PNe. Open circles show galactic objects classified as PNe, while triangles denote known symbiotic miras. Crosses denote the SMC PNe. Names of miras and suspected miras are labelled (Schmeja & Kimeswenger 2001).

which suggests that the ellipsoidal effect is the cause of the variability.

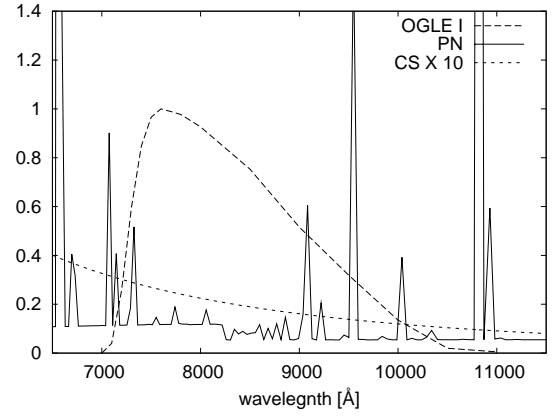


**Fig. 5.** OGLE I-band transmission curve and an example PN and CS spectrum.

#### 4.2. Binary fraction

One binary CSPN was found in the SMC sample of 45 PNe. This suggests that only about 2% of SMC PNe may be influenced by the CE phase, with the upper limit of about 7% (with 90% certainty, assuming 100% detection efficiency). This is lower than the binary fraction of 12 to 21% obtained for the Galactic Bulge (Miszalski et al. 2009a). However, the observed binary fraction in the SMC is subject to small statistics and strong selection effects, some of which may be distance dependent. Below we list and assess the influence of the selection effects.

To determine the binary fraction, the sample must be first corrected for the PN mimics. As explained in Section 2, all the PNe in the sample were spectroscopically confirmed. Usually the SMC PNe were identified on the basis of the presence of the [O III] 5007 Å line, lack of stellar continuum, and small angular dimensions (unresolved sources). Contamination of diffuse nebulae, Strömgren spheres in the interstellar medium, or compact H II regions is possible. About 10% of the sample show an [O III] 5007 Å/H $\alpha$  flux ratio of the order of unity and may be unresolved diffuse nebulae.

Detection of photometric variations is possible only when the stellar continuum contributes significantly to the total brightness of the object in the I-band. The nebular lines and continuum can produce the main or even the entire contribution in the I-band in many spatially unresolved SMC PNe, suppressing the amplitude of a binary central star. The HST observations showed that most of the SMC PNe do not exceed 1 arcsec in diameter (Stanghellini et al. 2003; Shaw et al. 2006) and would not be resolved in the OGLE images.

To assess the relative contribution of the stellar continuum to the total I-band flux of an unresolved PN, we used an exploratory PN model offered by the test suite distributed with the code Cloudy (Ferland et al. 1998). The model assumed that the 50,000 K blackbody spectrum excites the ionization bounded nebula with reduced elemental abundances. The OGLE I-band transmission curve is shown along with the central star and nebular spectrum in Figure 5. The [S III] 9069 and 9532 Å lines contribute to the calculated brightness of the object in the nonstandard OGLE I-band filter (Udalski et al. 2002). The total nebular contribution is six times higher than the contribution of the central star in the I-band (18.6 magnitude at the distance to the SMC). The nebular contribution would be much lower for a cooler central star and a density bounded PN.

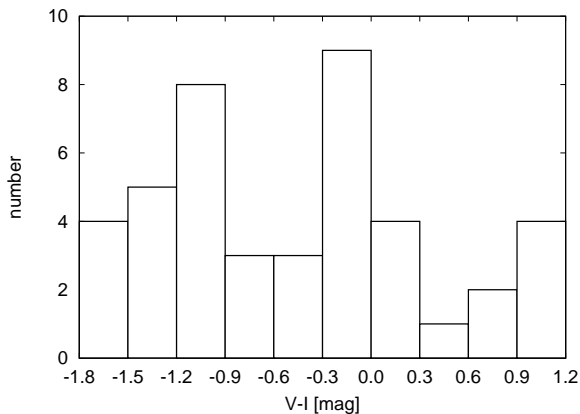


**Fig. 6.** Histogram of the V-I colours of all identified SMC PNe.

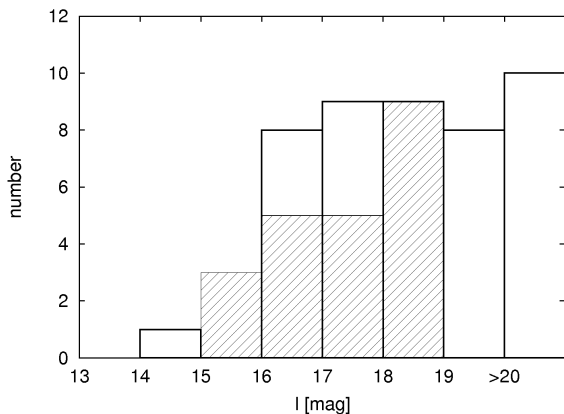


**Fig. 7.** Histogram of the I-band brightness of all identified SMC PNe. The hatched histogram of the binary CSPNe in the Galactic Bulge is overplotted (Miszalski et al. 2009a).

We plot the histogram of the  $V - I$  colours of the identified PNe in Figure 6. Most of the objects have colours different from  $-0.4$ , expected for unreddened CSPN (Ciardullo et al. 1999), even those for which the central star was easily detected in the HST observations. The diagram is only slightly affected by reddening (an average  $E(V - I)$  of 0.07 for the SMC, Haschke et al. 2011).

Central stars were detected in about 75% of the SMC PNe (Villaver et al. 2004). The nebular contribution could be significant in some of them. In 25% of cases no central star was detected, with the PN contributing all the light to the I-band. The inclusion of such objects in our sample can lower the derived binary fraction by about 25%.

The SMC CSPNe are expected to be fainter than their Galactic Bulge counterparts because of the difference in distance. This could lower the detection efficiency of the binary CSPNe. Assuming a similar intrinsic I-band brightness distribution of the SMC and the Galactic Bulge CSPNe populations, the observed distributions would be separated by about 4.7 mag. However, Galactic Bulge PNe are observed in the fields close to the Galactic centre, typically reddened by  $E(V - I)$  of 1 or more (Nataf et al. 2013) contrary to the only slightly reddened SMC PNe (Haschke et al. 2011). In addition, SMC PNe are more likely to be unresolved and contribute to the I-band brightness. This would reduce the separation of both distributions.

The distributions of the I-band brightness of the SMC PNe and the Galactic Bulge PNe known to harbour binary CSPNe

(Miszalski et al. 2009a) are compared in Figure 7. Bulge PNe are brighter on average only by about 1.5 mag from the SMC PNe, and their brightness distribution is much narrower. However, neither of the distributions can be treated as representative for the whole PN population. Very bright PNe, avoided by the OGLE-III pipeline, as well as very faint PNe may be underrepresented in the Galactic Bulge histogram. Some of the SMC PNe fall below the completeness limit of 21 mag for the OGLE-III survey in the I-band (Udalski et al. 2008).

The sensitivity of our search depends on the apparent brightness of the object and the data sampling. Only one object in our sample has fewer than 100 datapoints. More than half of the PNe identified in the SMC fields are fainter than 18 mag (Figure 7). However, the sensitivity limit for an 18 mag star observed 600 times is about 0.01 mag for a sinusoidal light curve. This is sufficient to detect most of the CSPNe with periods of up to 1-2 weeks, unless the binary system parameters were very unfavourable (De Marco et al. 2008). However, this requires at least one of the binary components to be observable at the distance to the SMC.

An M V type companion of the CSPN would be below the OGLE detection limit at the distance to the SMC (fainter than 26 mag in the I-band). Binary CSPNe discovered purely because of irradiation effects constitute almost half of the systems detected by Miszalski et al. (2009a). A detection of the CSPN binaries showing ellipsoidal variations and eclipsing binaries would be feasible, although the detection efficiency would be reduced by the nebular contribution.

Taking all the selection effects into account, the number of detected binaries toward the SMC may be reduced by 80% compared with that of the Galactic Bulge. The binary fraction corrected for the selection effects may be as high as 10% or higher.

#### 4.3. Period distribution

The period distribution of the binary CSPNe in the Galaxy has a maximum of about 0.4 day with only few systems with periods longer than one day (Miszalski et al. 2011). The distribution of the close WD-MS CSPNe binaries appears to agree well with the WD-MS post CE systems (Hillwig 2011). The latter distribution shows a lack of systems with periods longer than 5-10 days (Nebot Gómez-Morán et al. 2011).

The period of Jacoby SMC 1 is three to six times longer than the maximum of the distribution for binary CSPNe in the Galaxy. The probability of finding of a CSPN binary with such a long period is relatively low, but not negligible. We cannot rule out the possibility that this reflects the real difference in the period distributions for the Galactic and SMC binary CSPNe.

We cannot confirm whether Jacoby SMC 1 contains a WD-MS or a double degenerate binary. The period distribution for the Galactic double degenerate binaries may have maximum shorter than 0.4 day.

The post-CE period distribution depends primarily on the binding parameter  $\alpha_{CE}$  and the initial mass-ratio distribution. The cutoff for the periods above a few days in the distribution of the Galactic binary CSPNe suggests the  $\alpha_{CE} = 0.3$ , otherwise a tail towards longer orbital periods of up to 1000 days would be expected (Miszalski et al. 2009a). The binding parameter of an envelope of a giant star does not show a strong dependence with metallicity (Loveridge et al. 2011), thus  $\alpha_{CE}$  may be equal to 0.3 for the SMC as well.

The maximum of the period distribution depends on the assumed initial mass ratio. Zorotovic et al. (2011) have found that systems containing high-mass secondaries tend to have longer

post-CE orbital periods for a Galactic sample for post-CE binaries. The amplitude of the photometric variability increases with the secondary mass, but decreases with the orbital separation. Thus binaries with high-mass secondaries may have similar amplitudes (and the detection efficiency) to the systems with low-mass companions. It is unclear, however, why would the SMC binaries have more massive secondaries.

Reduced mass loss during the AGB phase may lead to somewhat more massive central stars of PNe (Villaver et al. 2007), but no correlation between the WD mass and the periods of the post-CE systems was found for CO-core WDs (Zorotovic et al. 2011).

## 5. Summary

We discovered only one binary CSPN in the SMC. The actual binary fraction of the CSPNe in the SMC may be similar to the value obtained for the Galactic Bulge PNe taking the selection effects into account. The sample is too small to derive firm conclusions concerning the period distribution of the post-CE binary CSPNe in the SMC.

In addition, observations allowed us to constrain the nature of some known PNe mimics. Three of them are probably Be stars and one is an YSO. The likelihood that [MA93] 22 is an optical counterpart of an Be/X-ray binary has increased. We discovered a new symbiotic star candidate.

*Acknowledgements.* This research has made use of the SIMBAD database, operated at CDS, Strasbourg, France. This work was financially supported by NCN of Poland through grants No. 2011/01/D/ST9/05966 and 719/N-SALT/2010/0. The OGLE project has received funding from the European Research Council under the European Community's Seventh Framework Programme (FP7/2007-2013)/ERC grant agreement no. 246678. Some of the observations reported in this paper were obtained with the Southern African Large Telescope (SALT), proposal 2012-1-POL-010, P.I. M. Hajduk. We thank the anonymous referee for the comments on the paper.

## References

- Belczyński, K., Mikołajewska, J., Munari, U., Ivison, R. J., & Friedjung, M. 2000, *A&AS*, 146, 407
- Boffin, H. M. J., Miszalski, B., Rauch, T., et al. 2012, *Science*, 338, 773
- Bolatto, A. D., Simon, J. D., Stanimirović, S., et al. 2007, *ApJ*, 655, 212
- Bond, H. E. 2000, in *Astronomical Society of the Pacific Conference Series*, Vol. 199, *Asymmetrical Planetary Nebulae II: From Origins to Microstructures*, ed. J. H. Kastner, N. Soker, & S. Rappaport, 115
- Boroson, T. A. & Liebert, J. 1989, *ApJ*, 339, 844
- Boyer, M. L., Srinivasan, S., van Loon, J. T., et al. 2011, *AJ*, 142, 103
- Ciardullo, R., Bond, H. E., Sipior, M. S., et al. 1999, *AJ*, 118, 488
- De Marco, O. 2009, *PASP*, 121, 316
- De Marco, O. 2011, in *Asymmetric Planetary Nebulae 5 Conference*
- De Marco, O., Hillwig, T. C., & Smith, A. J. 2008, *AJ*, 136, 323
- Evans, C. J., Howarth, I. D., Irwin, M. J., Burnley, A. W., & Harries, T. J. 2004, *MNRAS*, 353, 601
- Ferland, G. J., Korista, K. T., Verner, D. A., et al. 1998, *PASP*, 110, 761
- Greenstein, J. L. & Sargent, A. I. 1974, *ApJS*, 28, 157
- Haberl, F. & Sasaki, M. 2000, *A&A*, 359, 573
- Hajduk, M., Zijlstra, A. A., & Gesicki, K. 2011, in *Asymmetric Planetary Nebulae 5 Conference*
- Haschke, R., Grebel, E. K., & Duffau, S. 2011, *AJ*, 141, 158
- Henize, K. G. 1956, *ApJS*, 2, 315
- Henize, K. G. & Westerlund, B. E. 1963, *ApJ*, 137, 747
- Hillwig, T. C. 2011, in *Asymmetric Planetary Nebulae 5 Conference*
- Jacoby, G. H. 1980, *ApJS*, 42, 1
- Jacoby, G. H. & De Marco, O. 2002, *AJ*, 123, 269
- Jones, D., Pollacco, D., Faedi, F., & Lloyd, M. 2011, in *Asymmetric Planetary Nebulae 5 Conference*, 111P
- Leisy, P. & Dennefeld, M. 2006, *A&A*, 456, 451
- Lenz, P. & Breger, M. 2005, *Communications in Asteroseismology*, 146, 53
- Lindsay, E. M. 1961, *AJ*, 66, 169
- Loveridge, A. J., van der Sluys, M. V., & Kalogera, V. 2011, *ApJ*, 743, 49
- Lutz, J., Fraser, O., McKeever, J., & Tugaga, D. 2010, *PASP*, 122, 524
- Mennickent, R. E., Pietrzyński, G., Gieren, W., & Szewczyk, O. 2002, *A&A*, 393, 887
- Meyssonnier, N. 1995, *A&AS*, 110, 545
- Meyssonnier, N. & Azzopardi, M. 1993, *A&AS*, 102, 451
- Miszalski, B., Acker, A., Moffat, A. F. J., Parker, Q. A., & Udalski, A. 2009a, *A&A*, 496, 813
- Miszalski, B., Acker, A., Parker, Q. A., & Moffat, A. F. J. 2009b, *A&A*, 505, 249
- Miszalski, B., Corradi, R. L. M., Jones, D., et al. 2011, in *Asymmetric Planetary Nebulae 5 Conference*
- Morgan, D. H. 1995, *A&AS*, 112, 445
- Morgan, D. H. & Good, A. R. 1985, *MNRAS*, 213, 491
- Naik, S., Mathew, B., Banerjee, D. P. K., Ashok, N. M., & Jaiswal, R. R. 2012, *Research in Astronomy and Astrophysics*, 12, 177
- Nataf, D. M., Gould, A., Fouqué, P., et al. 2013, *ApJ*, 769, 88
- Nebot Gómez-Morán, A., Gänsicke, B. T., Schreiber, M. R., et al. 2011, *A&A*, 536, A43
- Oliveira, J. M., van Loon, J. T., Sloan, G. C., et al. 2013, *MNRAS*, 428, 3001
- Sanduleak, N., MacConnell, D. J., & Philip, A. G. D. 1978, *PASP*, 90, 621
- Sanduleak, N. & Pesch, P. 1981, *PASP*, 93, 431
- Schmeja, S. & Kimeswenger, S. 2001, *A&A*, 377, L18
- Schwarzenberg-Czerny, A. 1996, *ApJ*, 460, L107
- Shaw, R. A., Stanghellini, L., Villaver, E., & Mutchler, M. 2006, *ApJS*, 167, 201
- Skrutskie, M. F., Cutri, R. M., Stiening, R., et al. 2006, *AJ*, 131, 1163
- Stanghellini, L., Shaw, R. A., Balick, B., et al. 2003, *ApJ*, 596, 997
- Udalski, A., Kubiak, M., & Szymanski, M. 1997, *Acta Astron.*, 47, 319
- Udalski, A., Soszyński, I., Szymański, M. K., et al. 2008, *Acta Astron.*, 58, 329
- Udalski, A., Szymanski, M., Kubiak, M., et al. 2002, *Acta Astron.*, 52, 217
- Villaver, E., Stanghellini, L., & Shaw, R. A. 2004, *ApJ*, 614, 716
- Villaver, E., Stanghellini, L., & Shaw, R. A. 2007, *ApJ*, 656, 831
- Zorotovic, M., Schreiber, M. R., Gänsicke, B. T., et al. 2011, *A&A*, 536, L3